

Quenching the Kitaev honeycomb model

L. Rademaker^{1*}

¹ Perimeter Institute for Theoretical Physics, Waterloo, Ontario N2L 2Y5, Canada

* louk.rademaker@gmail.com

June 22, 2022

Abstract

I studied the non-equilibrium response of an initial Néel state under time evolution with the Kitaev honeycomb model. This time evolution can be computed using a random sampling over all relevant flux configurations. With isotropic interactions the system quickly equilibrates into a steady state valence bond solid. Anisotropy induces an exponentially long prethermal regime whose dynamics are governed by an effective toric code. Signatures of topology are absent, however, due to the high energy density nature of the initial state.

Contents

1	Introduction	1
2	Model, initial state and method	2
3	Results	4
3.1	Prethermalization	4
3.2	Steady state valence bond solid	7
4	Conclusion	8
A	Matter Hamiltonian time evolution	9
B	Diagonal ensemble	11
	References	12

1 Introduction

Quantum spin liquids [1] are intriguing forms of matter characterized by massive long-range entanglement. A defining feature is that they cannot be transformed adiabatically into non-entangled product states. One might wonder whether these opposite extremes can be connected under a *rapid* change of external parameters.

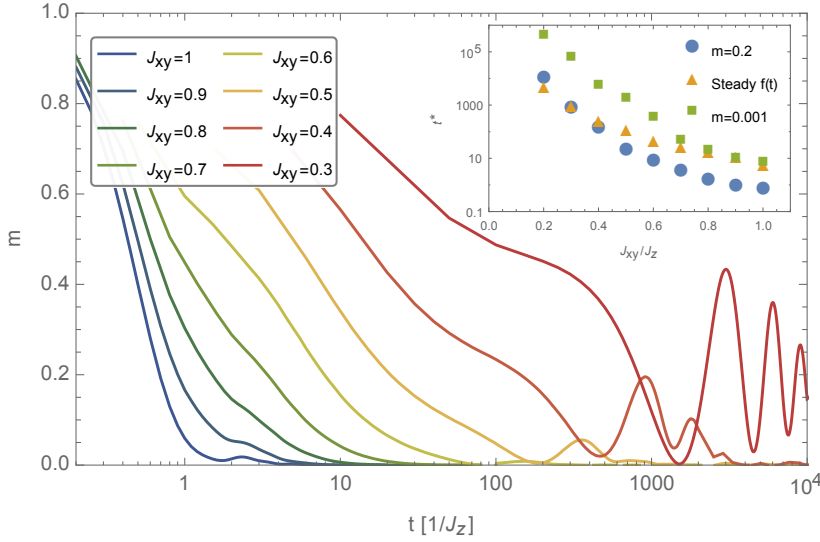


Figure 1: The staggered magnetization $m = (-1)^i \langle \sigma_i^z(t) \rangle$ after the quench for various J_{xy} , fixed $J_z = 1$, $N_{mc} = 2000$, and system size $L = 8$. While the magnetization vanishes quickly in the isotropic model, the response is exponentially slower when $J_{xy} < 1$. *Inset:* Typical timescales as a function of anisotropy. Shown here are the times it takes for the system to lose 80% and 99.9% of its staggered magnetization, as well as the time where the free energy density reaches its steady state value.

Such a rapid change is known as a quench [2, 3], and this set-up has led to the prediction and observation of dynamical phase transitions. [4, 5] As for spin liquids, under certain conditions topological order may survive time evolution with a non-topological Hamiltonian [6]. In this work, I will study the reverse question: can we find signatures of topology starting from a product state?

The Kitaev honeycomb model [7] provides an ideal playground to answer this question since it is exactly solvable. A slow ramp in this model has been studied before [8, 9], but this was completely within the space of the topological states. Here, I start from an antiferromagnetic Néel state, which can be expressed as a superposition of all possible flux configurations. I will show that the Néel state under time evolution with the Kitaev Hamiltonian will reach a steady state valence bond solid. Most surprisingly, an exponentially long prethermal regime appears when the interactions are anisotropic, as seen for example in the time evolution of the magnetization (Fig. 1). This prethermal regime is governed by an effective toric code, though the highly excited nature of the state makes identifying topological features difficult.

2 Model, initial state and method

Before presenting the results in detail, let me introduce the set-up of the quench. Consider spin- $\frac{1}{2}$ degrees of freedom σ_i on a honeycomb lattice. The unit cell has two sites, which I will label as the A and B site, shown in Fig. 2. The initial state will be a perfect Néel state polarized along the z -direction, which is an unentangled product state $|\psi_0\rangle = \prod_i |\uparrow_{iA}\rangle \otimes |\downarrow_{iB}\rangle$. Starting from this initial state I will compute the time evolution using the Kitaev honeycomb

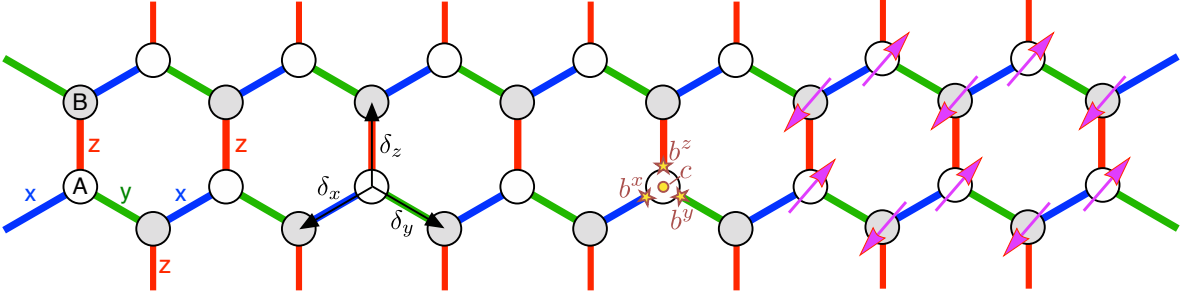


Figure 2: The Kitaev honeycomb model on a lattice. The unit cell with sites A and B is shown, together with the three inequivalent bonds labeled $\alpha = x, y, z$. The vectors δ_α indicate the nearest neighbor position relative to an A site. In the middle of the lattice I indicate how a spin can be split up into four Majorana operators b^α and c . On the right a visualization of the initial Néel state.

model. In this model the bonds between lattice sites are divided into three types, depending on their direction, as shown in Fig. 2. Each bond-type has an Ising spin interaction along a different spin orientation,

$$H = \sum_i J_x \sigma_{iA}^x \sigma_{i+\delta_x, B}^x + J_y \sigma_{iA}^y \sigma_{i+\delta_y, B}^y + J_z \sigma_{iA}^z \sigma_{iB}^z. \quad (1)$$

Kitaev's genius was his realization that one can solve this model exactly by representing each spin by four Majorana operators b^x, b^y, b^z and c . This enlarges the Hilbert space, and in the enlarged Hilbert space we can define 'enlarged' spin operators $\tilde{\sigma}^x = ib^x c, \tilde{\sigma}^y = ib^y c$, and $\tilde{\sigma}^z = ib^z c$. The projection operator onto the real, physical, subspace is $P = \frac{1}{2}(1 + b^x b^y b^z c)$. Therefore, the physical spins are given by $\sigma^\alpha = P \tilde{\sigma}^\alpha P$, which implies $\sigma^x = \frac{i}{2}(b^x c - b^y b^z), \sigma^y = \frac{i}{2}(b^y c - b^z b^x)$, and $\sigma^z = \frac{i}{2}(b^z c - b^x b^y)$. In the following, I will use that within the physical subspace, the real spins can also be represented by the operators of the form $\sigma^z = -ib^x b^y$ and similar expressions hold for σ^x and σ^y .

In terms of the new Majorana operators, the Hamiltonian reads

$$H = i \sum_{j, \alpha} J_\alpha u_{j\alpha} c_{jA} c_{j+\delta_\alpha, B} \quad (2)$$

where j sums over unit cells and $u_{j\alpha} = ib_{jA}^\alpha b_{j+\delta_\alpha, B}^\alpha = \pm 1$ is a static Z_2 gauge field living on the $\alpha = x, y, z$ bond. The product of Z_2 gauge fields along a plaquette is gauge-invariant and is the 'flux' $w_p = \sigma_1^x \sigma_2^y \sigma_3^z \sigma_4^x \sigma_5^y \sigma_6^z$. The remaining c -Majorana's are called 'matter' and are noninteracting.

The spin liquid ground state of the Kitaev honeycomb model is in the zero-flux sector, meaning all gauge fields $u_{j\alpha}$ are the same. In contrast, the Néel state, when expressed in terms of gauge and matter fields, is in a superposition of all possible flux configurations since $\langle \psi_0 | w_p | \psi_0 \rangle = 0$ where w_p is the plaquette flux operator.

A good basis to describe the Neel state is by pairing the remaining matter Majorana's along the z -bonds within one unit cell, $v_j = ic_{jA} c_{jB} = \pm 1$. Any possible state in the enlarged Hilbert space can be written as a superposition of u, v -configurations, $|\psi\rangle = \sum_{\{u_{j\alpha}, v_j\}} c_{\{u_{j\alpha}, v_j\}} |\{u_{j\alpha}, v_j\}\rangle$, and our task is to find the weight constants $c_{\{u_{j\alpha}, v_j\}}$. The fact that the Neel state is physical

and therefore must satisfy $P_j|\psi_0\rangle = |\psi_0\rangle$, and that it is an eigenstate of σ_j^z for every j , leads to two constraints on the possible u, v -configurations. On a lattice consisting of $L_x \times L_y$ unit cells with periodic boundary conditions, we have periodic chains of xy -bonds. The product of all $2L_x$ z -spins along such a xy -chain equals (-1) times the product of all x and y gauge fields. Therefore, this product of gauge fields must equal $(-1)^{L_x+1}$. Consequently, the Néel state is an equal-weight superposition of all $N_c = 2^{3L_x L_y - L_y}$ possible $u_{j\alpha}$ gauge field configurations that satisfy this constraint. The matter content v_i is fixed by the constraint $\sigma_{jA}^z \sigma_{jB}^z = -1$ within each unit cell, which implies $u_{jz} = v_j$. The relative phases between different $\{u_{j\alpha}, v_j\}$ -configurations are fixed by the expectation value of σ_j^z operators, and are multiples of i .

Having established how to represent the Néel state in the gauge-matter basis, I will briefly describe how to compute expectation values of time-evolved spin operators. Because the gauge fields are integrals of motion only the matter fields will be changing over time,

$$|\psi(t)\rangle = \frac{1}{\sqrt{N_c}} \sum_{\{u_{j\alpha}\}} |\{u_{j\alpha}\}\rangle \otimes e^{-iH^{\{u_{j\alpha}\}}t} |\psi_0^{\{u_{j\alpha}\}}\rangle \quad (3)$$

where $\{u_{j\alpha}\}$ represents a gauge field configuration that respects the aforementioned constraints, $|\psi_0^{\{u_{j\alpha}\}}\rangle$ is the initial matter field configuration determined by $v_j = u_{jz}$ and $H^{\{u_{j\alpha}\}}$ is a free matter Majorana Hamiltonian with hoppings depending on the Z_2 gauge fields. The magnetization on an A lattice site $m_{jA}(t) = \langle \psi(t) | \sigma_{jA}^z | \psi(t) \rangle$ can be found using the gauge-field-only representation of spin, $\sigma_{jA}^z = -ib_j^x b_j^y$. Therefore, the magnetization can be written as the return amplitude with *two* matter Hamiltonians,

$$m(t) = \frac{1}{N_c} \sum_{\{u_{j\alpha}\}} \langle \psi_0^{\{u_{j\alpha}\}} | e^{iH^{\{u'_{j\alpha}\}}t} e^{-iH^{\{u_{j\alpha}\}}t} | \psi_0^{\{u_{j\alpha}\}} \rangle \quad (4)$$

where the configurations $\{u'_{j\alpha}\}$ and $\{u_{j\alpha}\}$ differ only by the flip of the two gauge fields u_j^x and u_j^y . The sum over exponentially many gauge field configurations can be replaced by a random Monte Carlo sampling over all configurations [10, 11] that satisfy the constraints relevant for the initial Néel state. For each such configuration I need to compute these generalized return amplitudes for the matter Hamiltonian, which can be done efficiently using the Balian-Brezin decomposition as outlined in the supplementary information.¹ [12, 13] Note that an alternative way of deriving my results is by using the 'brick wall'-representation of the Kitaev honeycomb model. [14]

3 Results

3.1 Prethermalization

Since we are quenching through a quantum critical point, one would expect to find signatures of a dynamical phase transition as seen in the transverse field Ising model. [4, 5] To study this, I computed the nonequilibrium free energy density $f(t) = -\frac{1}{N} \log |\mathcal{G}(t)|$ associated with the return amplitude $\mathcal{G}(t) = \langle \psi(t) | \psi_0 \rangle$, and $N = L_x L_y = L^2$. The results are shown in Fig. 3. Despite clear system-size independent results, there is no nonanalytic behavior observed for

¹See Online Supplementary Information.

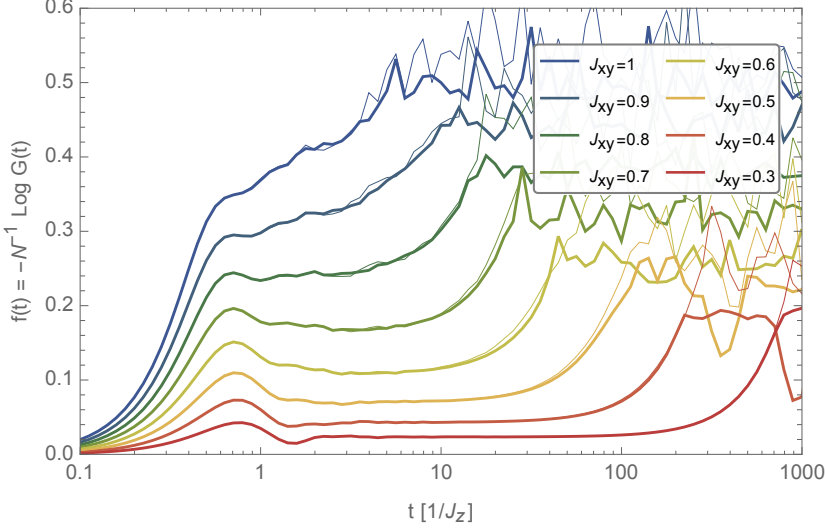


Figure 3: The nonequilibrium free energy $f(t) = -\frac{1}{N} \log \mathcal{G}(t)$ for various J_{xy} , fixed $J_z = 1$, $N_{mc} = 20000$, and system sizes $L = 6$ (thin lines) and $L = 8$ (thick lines), where $L_x = L_y = L$. No dynamical phase transition is observed in the short times before a steady state plateau emerges. A prethermalization regime appears with increasing anisotropy.

short times. In the isotropic case, the free energy smoothly increases to a steady state value within a timescale of order unity, after which there are system-size dependent fluctuations around this steady-state value. Due to these fluctuations, it is currently not possible to see whether there is a dynamical phase transition at the onset of the fluctuation window.

However, upon increasing the anisotropy J_{xy}/J_z , where $J_x = J_y \equiv J_{xy}$, a plateau emerges that can last exponentially long in the inverse magnetic coupling strength $1/J_z$. This is reminiscent of *prethermalization* [15–20] that occurs in systems close to integrability. A similarly slow response as a function of anisotropy can be observed in the staggered magnetization $m(t) = \sum_j (-1)^j \langle \sigma_j^z(t) \rangle$, shown in Fig. 1 and Fig. 4. For example, a factor of 5 increase in the anisotropy leads to a factor 10^5 in slowing down before the magnetization has practically vanished. Different measures of a typical time-scale, namely the onset of the free energy plateau or when the magnetization reaches a 0.2 or 0.001 threshold, all display an approximately exponential dependence on the anisotropy $t^* \sim e^{cJ_z/J_{xy}}$.

We thus find the emergence, for the anisotropic model, of a distinct prethermalized regime. This can be understood using the framework of Ref. [18]. The anisotropic Kitaev Hamiltonian can be written as $H = J_z N + J_{xy} Y$ where N is the sum of local commuting terms with integer eigenvalues and $[N, Y] \neq 0$. For $J_{xy} < J_z$, we can perform a unitary transformation such that $H = -J_z N + D + \mathcal{O}(e^{-J_z/J_{xy}})$ where $[N, D] = 0$. Consequently, for an exponentially long time $N + D$ acts as an effective conserved quantity. In practice this means that the relative spin-orientation along the z -bonds remains fixed. The existence of such a spin-lock can be confirmed by measuring the static spin correlation function $S_{ij}^{zz}(t) = \langle \psi(t) | \sigma_i^z \sigma_j^z | \psi(t) \rangle$. As shown in Fig. 5, even in the isotropic case the relative orientation of spins along a z -bond remains nonzero in the infinite time-limit. This can be further corroborated by computing the static spin correlations in the diagonal ensemble, which indeed yields a steady state with zero magnetization but nonzero spin correlations along the z -bond. Notice that other static

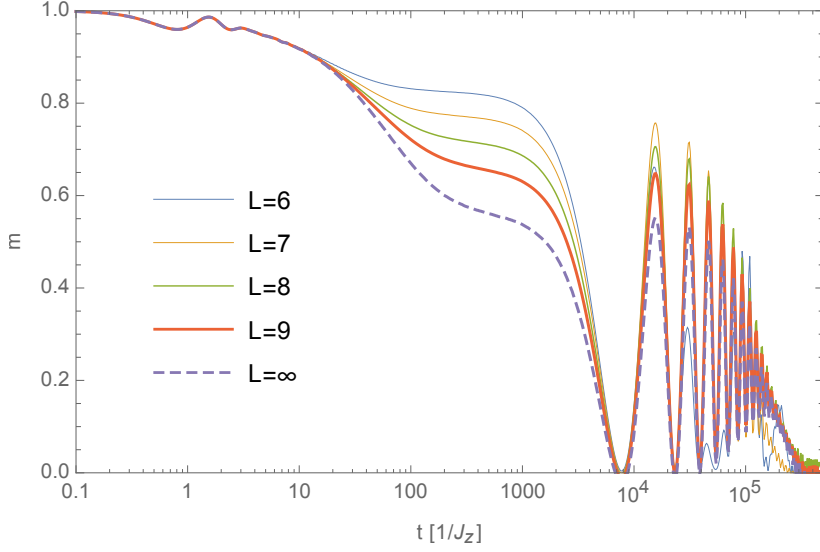


Figure 4: In case of large anisotropy the decay of magnetization is extremely slow, here shown for $J_{xy} = 0.2J_z$ with $N_{mc} = 2000$ and various system sizes extrapolated to $L = \infty$. Between $t_1 \sim 1$ and $t_2 \sim 10^{3.5} J_z^{-1}$ there is a persisting magnetization, due to the high return amplitude visible in Fig. 3. After this the system is dominated by large magnetization oscillations that finally disappear around $t_3 \sim 10^{5.5} J_z^{-1}$.

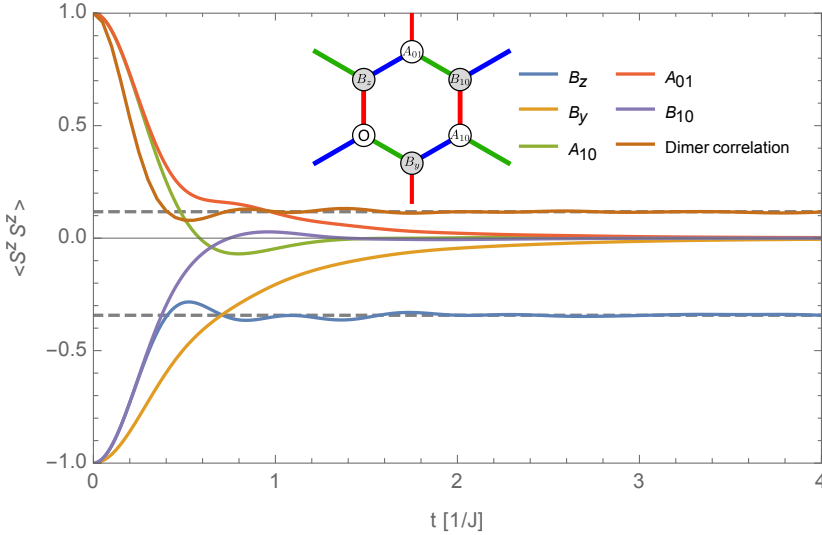


Figure 5: The static spin-spin correlations $\langle \sigma_i^z \sigma_j^z \rangle$ for various short-range spins, in the isotropic model, with $L = 8$ and $N_{mc} = 2000$. After a short time all spin correlations vanish except the nearest-neighbor correlation along a z -bond. The long-range dimer-dimer correlation function, here measured at the longest possible distance between two sets of z -bonds, also obtains a nonzero steady state value. These correlations are indicative of a valence bond solid phase.

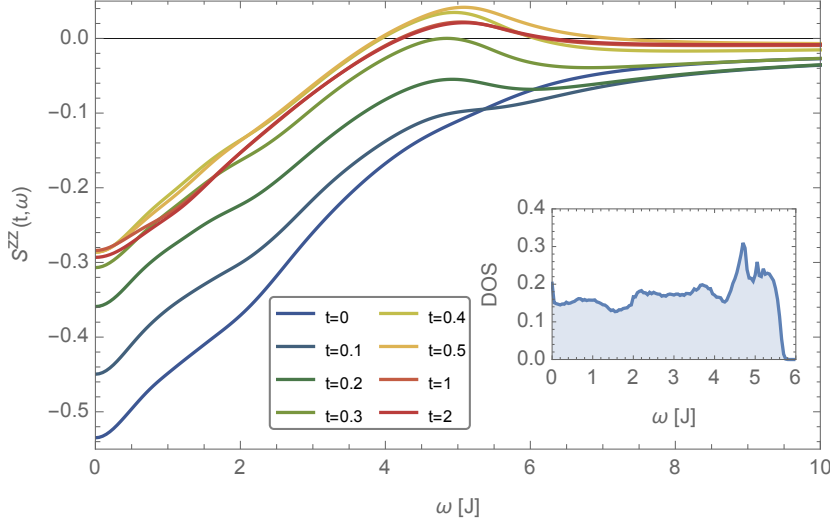


Figure 6: The dynamical two-time response in the isotropic quench, as a function of frequency ω for various waiting times t . Directly after the quench ($t = 0$) the system displays a Drude-like peak associated with the Néel order. The Drude peak is suppressed as time progresses, consistent with the loss of magnetization, see Fig. 1. After $t \sim 0.3J^{-1}$ the Drude peak remains constant, and a dynamic magnetization reversal occurs in the frequency range between 4 – 6 J, where the flux-averaged Majorana density of states (see inset) is highest and corresponding to the triplet excitation in the valence-bond solid.

spin correlations vanish.

Given this spin-lock an approximate Hamiltonian can be constructed that preserves the relative orientation of the spins along a z -bond, which was actually done in the original work of Kitaev [7]. The effective Hamiltonian, after a suitable local unitary transformation, describes a toric code. [21] The prethermal regime can therefore be understood as a high-temperature phase of the toric code. Signatures of topology, such as anyonic excitations, are therefore difficult to see since they are defined only close to the ground state.

3.2 Steady state valence bond solid

In the isotropic case there is no signature of prethermalization and after a short time of order unity the system equilibrates. While there is zero net staggered magnetization in this steady state, there are remnant nearest-neighbor spin correlations along the z -bond. Furthermore, the dimer-dimer correlation function $D_{ij}^{zz}(t) = \langle \sigma_i^z \sigma_{i+\delta_z}^z \sigma_j^z \sigma_{j+\delta_z}^z \rangle$ [22] function displays long-range order as shown in Fig. 5. This suggests the steady state is a valence bond solid with the singlets oriented along the z -bonds. Notice that this state does break rotational invariance, since the singlet bonds live on the z -bonds which are inequivalent to the x, y -bonds of the lattice.

Another way to quantify the steady state is through the dynamic two-time spin correlation function $S_j^{zz}(t, t') = \langle \psi(t) | \sigma_{jA}^z(t') \sigma_{jB}^z | \psi(t) \rangle$. [23–25] As shown in Fig. 6, the initial $t = 0$ dynamical response can be understood in terms of a Drude peak at zero frequency. The area of the low-frequency peak corresponds to the magnitude of the antiferromagnetic correlations along a z -bond. At later times this correlations gets suppressed in the frequency range between

0 and $6J$, which is the flux-averaged bandwidth of the matter Majorana's. Interestingly, for times $t > 0.5$ a reversal of the dynamic correlations for $4J < \omega < 6J$ appears. This is a signature of the elementary triplet excitation of the valence bond solid.

We thus find a dynamic crossover from a Néel state to a valence bond solid. This transition in equilibrium is known as a deconfined quantum phase transition and falls outside the usual Landau classification of continuous phase transitions. [26] The absence of any finite time singularity is due to the fact that the location of the valence bonds are determined by the orientation of the initial Néel state. There is no dynamical spontaneous symmetry breaking: a Néel state polarized along the x -axis would give rise to a valence bond solid with singlets along the x -bonds, and so forth. It is an interesting open question to study what happens when an initial Néel state is not aligned along one of the principal spin axes.

4 Conclusion

I showed that starting from a Néel state, time evolution with the Kitaev honeycomb model leads to a steady state valence bond solid. When the interactions are anisotropic, an exponentially long prethermal regime appears whose dynamics can be effectively described by a toric code. Even though the intermediate dynamics are governed by a toric code Hamiltonian, there are no signatures of topology or anyonic excitations because the state is highly excited. Further study is warranted on the high-temperature regime of the toric code to understand the precise nature of this regime.

To what extent these results remain valid beyond the exactly solvable model, for example by introducing a small Heisenberg term, is an open question. Based on the proof of Ref. [18] I expect that the prethermal regime will persist even in the presence of such perturbations, but quantifying this requires new computational techniques beyond the ones used in this work.

A interesting aspect that was not included in this study is the dynamics of entanglement. In the Kitaev honeycomb model, the ground state has nontrivial entanglement entropy [27, 28] and it is interesting to see whether and how such a nontrivial entanglement can arise dynamically.

Finally, in recent years some material systems have been proposed to be experimental realizations of the Kitaev honeycomb model [29]. Though straining these materials is unlikely to give rise to the desired anisotropy to observe a prethermal regime, it might be possible to chemically engineer these system to get the anisotropic interactions desired. It will also be interesting to see the dynamic response after a quench with an initial state resembling the spiral magnetic order found in these materials. [30,31]

Acknowledgements

We thank Tim Hsieh, Khadijeh (Sona) Najafi, Leon Balents, Hae-Young Kee and Yong Baek Kim for useful discussions.

Funding information This research was supported by Perimeter Institute for Theoretical Physics. Research at Perimeter Institute is supported by the Government of Canada through the Department of Innovation, Science and Economic Development Canada and by

the Province of Ontario through the Ministry of Research, Innovation and Science.

A Matter Hamiltonian time evolution

As described in the main text, the time evolution of the Kitaev honeycomb model is completely due to the Majorana fermions. In each unit cell j , which contains a z -link, we identify an A and B sublattice site. The c -Majorana's in Kitaev's notation are then paired along the z -link to form complex fermions,

$$c_{jA} = a_j + a_j^\dagger, \quad (5)$$

$$c_{jB} = -i(a_j - a_j^\dagger). \quad (6)$$

The matter Hamiltonian on the full honeycomb lattice reads

$$H^{\{u\}} = - \sum_j \left\{ (J_z u_j^z) (2a_j^\dagger a_j - 1) + (J_x u_j^x) (a_j + a_j^\dagger) (a_{j+\delta_x} - a_{j+\delta_x}^\dagger) + (J_y u_j^y) (a_j + a_j^\dagger) (a_{j+\delta_y} - a_{j+\delta_y}^\dagger) \right\} \quad (7)$$

where j labels a unit cell, and δ connects to the unit cell with center at position $\delta_x = \frac{1}{2}(-\sqrt{3}\hat{x} - 3\hat{y})$, and $\delta_y = \frac{1}{2}(\sqrt{3}\hat{x} - 3\hat{y})$.

In each gauge sector, the required initial state is the product state where unit cells with $u_j^z = 1$ are occupied with a complex matter fermion. For later purposes it is practical to perform a particle-hole transformation on 'occupied' sites, so that the Hamiltonian becomes

$$H^{\{u\}} = \sum_j \left\{ J_z (2a_j^\dagger a_j - 1) + (J_x u_{j+\delta_x}^z u_j^x) (a_j + a_j^\dagger) (a_{j+\delta_x} - a_{j+\delta_x}^\dagger) + (J_y u_{j+\delta_y}^z u_j^y) (a_j + a_j^\dagger) (a_{j+\delta_y} - a_{j+\delta_y}^\dagger) \right\}. \quad (8)$$

With the Hamiltonian Eqn. (8), the initial matter state is nothing but the a -vacuum $|0\rangle$, defined by $a_j|0\rangle = 0$. This matter Hamiltonian can be brought into a canonical Bogoliubov-De Gennes (BdG) format,

$$H^{\{u_{j\alpha}\}} = \frac{1}{2} \begin{pmatrix} \mathbf{a}^\dagger & \mathbf{a} \end{pmatrix} \begin{pmatrix} H_d & \Delta \\ -\Delta & -H_d \end{pmatrix} \begin{pmatrix} \mathbf{a} \\ \mathbf{a}^\dagger \end{pmatrix} \quad (9)$$

where H_d is a real-valued symmetric matrix, Δ a real-valued antisymmetric matrix, and the vector $\begin{pmatrix} \mathbf{a}^\dagger & \mathbf{a} \end{pmatrix}$ contains all creation and annihilation operators for all unit cells. The $2N \times 2N$ BdG matrix in Eqn. (9) can be diagonalized, $H_{BdG} = V\Lambda V^\dagger$, with real eigenvalues $\Lambda = \text{diag}(\epsilon_1, \epsilon_2, \dots, \epsilon_N, -\epsilon_1, \dots, -\epsilon_N)$ and V a real orthogonal matrix of the form $V = \begin{pmatrix} Q & R \\ R & Q \end{pmatrix}$. This diagonalization allows us to compute the Balian-Brezin decomposition of the time evolution operator, [12, 13]

$$e^{-iHt} = e^{\frac{1}{2}a^\dagger X a^\dagger} e^{a^\dagger Y a} e^{\frac{1}{2}a Z a} \det \left[R e^{-i\Lambda t/2} + Q e^{i\Lambda t/2} \right] \quad (10)$$

where $A = Q e^{i\Lambda t} Q^\dagger + R e^{-i\Lambda t} R^\dagger$, $B = Q e^{-i\Lambda t} R^\dagger + R e^{i\Lambda t} Q^\dagger$, $X = B A^{-1}$, $e^{-Y^\dagger} = A$, and $Z = A^{-1} B^*$.

The simplest quantity to compute is the overlap of the initial state with the time-evolved state, known as the return amplitude $\mathcal{G}(t) = \langle \psi(t) | e^{-iHt} | \psi_0 \rangle$. Because different flux sectors are orthogonal to one another, the total return amplitude is a sum of matter Majorana return amplitudes in each gauge sector,

$$\mathcal{G}(t) = \frac{1}{N_c} \sum_{\{u_{j\alpha}\}} \langle \psi_0^{\{u_{j\alpha}\}} | e^{-iH^{\{u_{j\alpha}\}} t} | \psi_0^{\{u_{j\alpha}\}} \rangle. \quad (11)$$

Note that due to the particle-hole transformation, the state $|\psi_0^{\{u_{j\alpha}\}}\rangle$ is equal to the a -vacuum, so $a_j |\psi_0^{\{u_{j\alpha}\}}\rangle = 0$ for every a_j . To simplify notation, from now on I will write $|0\rangle$ for the initial state.

The return amplitude for a single free Majorana Hamiltonian follows directly from the Balian-Brezin decomposition Eqn. (10),

$$\langle 0 | e^{-iH^{\{u_{j\alpha}\}} t} | 0 \rangle = \det \left[R e^{-i\Lambda t/2} + Q e^{i\Lambda t/2} \right]. \quad (12)$$

Since the number of gauge field configurations scales exponentially with system size, it is impossible to compute the above sum of Eqn. (11) exactly. Instead, I averaged over N_{mc} random gauge field configurations that satisfy the constraints set by the initial state. It turns out that $N_{mc} = 1000$ yields sufficient accuracy for the system sizes considered.

The staggered magnetization, defined as $m(t) = \frac{1}{2N} \sum_j \langle \psi(t) | \sigma_{jA}^z - \sigma_{jB}^z | \psi(t) \rangle$, will decay over time starting from $m(t=0) = 1$. Using the representation $\sigma_{jA}^z = -i b_j^x b_j^y$, valid within the physical subspace, we see that the magnetization can be computed as a sum over return amplitudes involving two Hamiltonians,

$$R_2(t) = \langle 0 | e^{iH_2 t} e^{-iH_1 t} | 0 \rangle \quad (13)$$

where H_1 and H_2 only differ through a flip of the u_{jx} and u_{jy} gauge fields neighboring the spin that we want to measure. I proceed by making the Balian-Brezin decomposition for both H_1 and H_2 ,

$$\mathcal{R}(t) = \det \left[R_2 e^{i\Lambda_2 t/2} + Q_2 e^{-i\Lambda_2 t/2} \right] \det \left[R_1 e^{-i\Lambda_1 t/2} + Q_1 e^{i\Lambda_1 t/2} \right] \langle 0 | e^{\frac{1}{2} a Z_2^* a} e^{\frac{1}{2} a^\dagger X_1 a^\dagger} | 0 \rangle. \quad (14)$$

The remaining part can be brought again in the Balian-Brezin form,

$$\langle 0 | e^{\frac{1}{2} a Z_2^* a} e^{\frac{1}{2} a^\dagger X_1 a^\dagger} | 0 \rangle = \sqrt{\det [Z_2^* X_1 + I]} \quad (15)$$

$$\begin{aligned} & \times \langle 0 | e^{\frac{1}{2} a^\dagger X_1 (Z_2^* X_1 + I)^{-1} a^\dagger} e^{a^\dagger (-\log(Z_2^* X_1 + I))^\top a} e^{\frac{1}{2} a (Z_2^* X_1 + I)^{-1} Z_2^*} | 0 \rangle \\ & = \sqrt{\det [Z_2^* X_1 + I]} \end{aligned} \quad (16)$$

The square root can be avoided by observing that both Z and X are skew-symmetric, and thus using the Sylvesters determinant lemma we find

$$\sqrt{\det [Z_2^* X_1 + I]} = \text{Pf} \left[\begin{pmatrix} X_1 & -I \\ I & Z_2^* \end{pmatrix} \right] \quad (17)$$

In conclusion, the Balian-Brezin decomposition yields for the return amplitude with two Hamiltonians

$$R_2(t) = \det [R_2 e^{i\Lambda_2 t/2} + Q_2 e^{-i\Lambda_2 t/2}] \det [R_1 e^{-i\Lambda_1 t/2} + Q_1 e^{i\Lambda_1 t/2}] \text{Pf} \left[\begin{pmatrix} X_1 & -I \\ I & Z_2^* \end{pmatrix} \right]. \quad (18)$$

Note that the static correlations $S_{ij}^{zz}(t) = \langle \psi(t) | \sigma_i^z \sigma_j^z | \psi(t) \rangle$ can be computed using the same formulæ, where now the gauge fields need to be flipped on the x, y -bonds adjacent to both sites i and j .

Finally, I can compute the dynamic two-time correlation function

$$S_{ij}^{zz}(t, t') = \langle \psi(t) | \sigma_i^z(t') \sigma_j^z | \psi(t) \rangle. \quad (19)$$

This requires the computation of a return amplitude of time evolution with three different Hamiltonians. Using repeatedly the Balian-Brezin trick this can be expressed as

$$R_3(t, t') = \langle 0 | e^{iH_3(t+t')} e^{-iH_2 t'} e^{-iH_1 t} | 0 \rangle \quad (20)$$

$$\begin{aligned} &= \det \left[R_3 e^{i\Lambda_3(t+t')/2} + Q_3 e^{-i\Lambda_3(t+t')/2} \right] \det \left[R_2 e^{-i\Lambda_2 t'/2} + Q_2 e^{i\Lambda_2 t'/2} \right] \\ &\quad \times \det \left[R_1 e^{-i\Lambda_1 t/2} + Q_1 e^{i\Lambda_1 t/2} \right] \\ &\quad \times \langle 0 | e^{\frac{1}{2} a Z_3^* a} e^{\frac{1}{2} a^\dagger X_2 a^\dagger} e^{a^\dagger Y_2 a} e^{\frac{1}{2} a Z_2 a} e^{\frac{1}{2} a^\dagger X_1 a^\dagger} | 0 \rangle \end{aligned} \quad (21)$$

$$\begin{aligned} &= \det \left[R_3 e^{i\Lambda_3(t+t')/2} + Q_3 e^{-i\Lambda_3(t+t')/2} \right] \left(\det \left[R_2 e^{-i\Lambda_2 t'/2} + Q_2 e^{i\Lambda_2 t'/2} \right] \right)^{-1} \\ &\quad \times \det \left[R_1 e^{-i\Lambda_1 t/2} + Q_1 e^{i\Lambda_1 t/2} \right] \\ &\quad \times \text{Pf} \left[\begin{pmatrix} X_2 & -I \\ I & Z_3^* \end{pmatrix} \right] \text{Pf} \left[\begin{pmatrix} Z_2 & -I \\ I & X_1 \end{pmatrix} \right] \\ &\quad \times \text{Pf} \left[\begin{pmatrix} ((Z_3^*)^{-1} + X_2)^{-1} & -A_2 \\ A_2 & (X_1^{-1} + Z_2)^{-1} \end{pmatrix} \right]. \end{aligned} \quad (22)$$

B Diagonal ensemble

The diagonal ensemble is defined as follows. Our initial state is given by $|\psi\rangle = \sum_n c_n |n\rangle$ where the $|n\rangle$ form an orthonormal set of eigenstates. Strictly speaking, the time evolution of our state is then $|\psi(t)\rangle = \sum_n c_n e^{-iE_n t} |n\rangle$. The diagonal ensemble is a density matrix composed of the time-independent diagonal of the initial state density matrix,

$$\rho_D = \sum_n |c_n|^2 |n\rangle \langle n|. \quad (23)$$

In our case, the eigenstates of our system have the form $|\{u\}\rangle \otimes |\{f\}\rangle$ where $|\{f\}\rangle$ are Fock states composed of the single-particle wavefunctions diagonalizing the matter BdG Hamiltonian. Since the flux sectors are orthogonal we can construct a diagonal ensemble within each flux sector. The trace carries over to the extended Hilbert space provided we use the physical subspace projector and our initial state is completely embedded in the physical subspace.

Any operator that changes the flux sector, such as an isolated σ_j^z , must have a zero expectation value in the diagonal ensemble. The only (possibly) nonzero expectation values of two-spin operators are of the form $\sigma_{jA}^z \sigma_{jB}^z$ along a z -bond. Using $\sigma_A^z \sigma_B^z = i b_A^z c_A i b_B^z c_B = -i u^z c_A c_B$, and the particle-hole transformation defined above, I find

$$\text{Tr} \sigma_{jA}^z \sigma_{jB}^z \rho_D = 1 - 2 \text{Tr} a_j^\dagger a_j \rho_D \quad (24)$$

$$= 1 - 2 \frac{1}{N_c} \sum_{\{u\}} \sum_{m=1}^L \left(Q_{jm} Q_{mj}^\dagger (R^\top R)_{mm} + R_{jm} R_{mj}^\dagger (Q^\top Q)_{mm} \right) \quad (25)$$

where I used the diagonalization of the matter Hamiltonian defined in the previous section.

References

- [1] L. Savary and L. Balents, *Quantum spin liquids: a review*, Rep. Prog. Phys. **80**(1), 016502 (2016).
- [2] A. Polkovnikov, K. Sengupta, A. Silva and M. Vengalattore, *Colloquium: Nonequilibrium dynamics of closed interacting quantum systems*, Rev. Mod. Phys. **83**(3), 863 (2011).
- [3] F. H. L. Essler and M. Fagotti, *Quench dynamics and relaxation in isolated integrable quantum spin chains*, J. Stat. Mech. **06**(6), 064002 (2016).
- [4] M. Heyl, A. Polkovnikov and S. Kehrein, *Dynamical Quantum Phase Transitions in the Transverse-Field Ising Model*, Phys. Rev. Lett. **110**(13), 135704 (2013).
- [5] P. Jurcevic, H. Shen, P. Hauke, C. Maier, T. Brydges, C. Hempel, B. P. Lanyon, M. Heyl, R. Blatt and C. F. Roos, *Direct Observation of Dynamical Quantum Phase Transitions in an Interacting Many-Body System*, Phys. Rev. Lett. **119**(8), 080501 (2017).
- [6] D. I. Tsomokos, A. Hamma, W. Zhang, S. Haas and R. Fazio, *Topological order following a quantum quench*, Phys. Rev. A **80**(6), 060302 (2009).
- [7] A. Kitaev, *Anyons in an exactly solved model and beyond*, Annals of Physics **321**(1), 2 (2006).
- [8] K. Sengupta, D. Sen and S. Mondal, *Exact Results for Quench Dynamics and Defect Production in a Two-Dimensional Model*, Phys. Rev. Lett. **100**(7), 077204 (2008).
- [9] S. Mondal, D. Sen and K. Sengupta, *Quench dynamics and defect production in the Kitaev and extended Kitaev models*, Phys. Rev. B **78**(4), P04010 (2008).
- [10] A. Smith, J. Knolle, D. L. Kovrizhin and R. Moessner, *Disorder-free localization*, arXiv p. arXiv:1701.04748 (2017), 1701.04748.
- [11] A. Smith, J. Knolle, R. Moessner and D. L. Kovrizhin, *Absence of Ergodicity without Quenched Disorder: from Quantum Disentangled Liquids to Many-Body Localization*, arXiv p. arXiv:1705.09143 (2017), 1705.09143.
- [12] R. Balian and E. Brezin, *Nonunitary bogoliubov transformations and extension of Wick's theorem*, Nuovo Cimento B (1965-1970) **64**(1), 37 (1969).
- [13] K. Najafi and M. A. Rajabpour, *On the possibility of complete revivals after quantum quenches to a critical point*, arXiv p. arXiv:1707.07178 (2017), 1707.07178.
- [14] H.-D. Chen and Z. Nussinov, *Exact results on the Kitaev model on a hexagonal lattice: spin states, string and brane correlators, and anyonic excitations*, Journal of Physics A: Mathematical and Theoretical **41**(7), 075001 (2008).
- [15] J. Berges, S. Borsányi and C. Wetterich, *Prethermalization*, Phys. Rev. Lett. **93**(14), 495 (2004).

- [16] P. Gagel, P. P. Orth and J. Schmalian, *Universal Postquench Prethermalization at a Quantum Critical Point*, Phys. Rev. Lett. **113**(22), 220401 (2014).
- [17] B. Bertini, F. H. L. Essler, S. Groha and N. J. Robinson, *Prethermalization and Thermalization in Models with Weak Integrability Breaking*, Phys. Rev. Lett. **115**(18), 180601 (2015).
- [18] D. Abanin, W. de Roeck, W. W. Ho and F. Huveneers, *A Rigorous Theory of Many-Body Prethermalization for Periodically Driven and Closed Quantum Systems*, Comm. Math. Phys. **354**(3), 809 (2017).
- [19] D. V. Else, P. Fendley, J. Kemp and C. Nayak, *Prethermal Strong Zero Modes and Topological Qubits*, arXiv p. arXiv:1704.08703 (2017), 1704.08703v1.
- [20] M. Marcuzzi, J. Marino, A. Gambassi and A. Silva, *Prethermalization in a Nonintegrable Quantum Spin Chain after a Quench*, Phys. Rev. Lett. **111**(19), 197203 (2013).
- [21] A. Kitaev, *Fault-tolerant quantum computation by anyons*, Annals of Physics **303**, 2 (2003).
- [22] A. W. Sandvik, *Evidence for Deconfined Quantum Criticality in a Two-Dimensional Heisenberg Model with Four-Spin Interactions*, Phys. Rev. Lett. **98**(22), 227202 (2007).
- [23] J. Knolle, D. L. Kovrizhin, J. T. Chalker and R. Moessner, *Dynamics of a Two-Dimensional Quantum Spin Liquid: Signatures of Emergent Majorana Fermions and Fluxes*, Phys. Rev. Lett. **112**(20), 207203 (2014).
- [24] F. Zschocke and M. Vojta, *Physical states and finite-size effects in Kitaev's honeycomb model: Bond disorder, spin excitations, and NMR lineshape*, Phys. Rev. B **92**, 014403 (2015).
- [25] J. Knolle, D. L. Kovrizhin, J. T. Chalker and R. Moessner, *Dynamics of fractionalization in quantum spin liquids*, Phys. Rev. B **92**(11), 225 (2015).
- [26] T. Senthil, A. Vishwanath, L. Balents, S. Sachdev and M. P. A. Fisher, *Deconfined Quantum Critical Points*, Science **303**(5), 1490 (2004).
- [27] H. Yao and X.-L. Qi, *Entanglement Entropy and Entanglement Spectrum of the Kitaev Model*, Phys. Rev. Lett. **105**(8), 080501 (2010).
- [28] B. Dóra and R. Moessner, *Gauge field entanglement of Kitaev's honeycomb model*, arXiv p. arXiv:1710.01926 (2017), 1710.01926v1.
- [29] G. Jackeli and G. Khaliullin, *Mott Insulators in the Strong Spin-Orbit Coupling Limit: From Heisenberg to a Quantum Compass and Kitaev Models*, Phys. Rev. Lett. **102**(1), 017205 (2009).
- [30] A. Biffin, R. D. Johnson, I. Kimchi, R. Morris, A. Bombardi, J. G. Analytis, A. Vishwanath and R. Coldea, *Noncoplanar and Counterrotating Incommensurate Magnetic Order Stabilized by Kitaev Interactions in γ -Li₂IrO₃*, Phys. Rev. Lett. **113**(19), 197201 (2014).

- [31] J. Chaloupka, G. Jackeli and G. Khaliullin, *Zigzag Magnetic Order in the Iridium Oxide Na_2IrO_3* , Phys. Rev. Lett. **110**(9), 097204 (2013).